Grenze International Journal of Engineering and Technology, June Issue

Geospatial Variation Analysis Utilising Image Processing Techniques on Satellite Data: A Case Study of Delhi and Kerala, India

Aishwarya N[1], Gowtham O R[2], Nandkishor J[3], Teja N Gowda[4] and Yuktha M Y[5]
[1]Assistant Professor, Department of Electronics & Communication Engineering, Dayananda Sagar College of Engineering, Bengaluru, Karnataka, India
Email: aishwaryan-ece@dayanandasagar.edu
[2-5]Student, Department of Electronics & Communication Engineering, Dayananda Sagar College of Engineering, Bengaluru, Karnataka, India
Email: gowtham05or@gmail.com, nandkishor.j0602@gmail.com, tejagowda975@gmail.com, yukthamy14@gmail.com

***Abstract*—Satellite imaging provides an abundant source of information needed to track and examine changes on the Earth's surface. Geospatial variation analysis aids in the identification of patterns, trends and anomalies across regions, which is helpful for urban planning, agriculture, disaster management, etc.**
As a proof-of-concept demonstration, this work shows how low-cost image processing techniques applied to Satellite image data open-sourced from the Landsat gallery can yield useful policy insights.
The findings, which align with Sustainable Development Goals (SDGs) 11, 13 and 15, support flood resilience planning in Kerala and urban green cover management in Delhi, without requiring sophisticated AI models or extensive ground data.

Index Terms— Geospatial changes, satellite image, Landsat, image processing, segmentation, SDGs.

I. INTRODUCTION

To visualise and understand the geographical distribution and linkages of different resources, such as infrastructure, social resources and natural resources, resource mapping utilising Geographic Information Systems (GIS) is essential.
It supports well-informed planning, management and decision-making in fields like resource allocation, urban planning, environmental protection and disaster response. However, resource mapping through surveying is labour-intensive, particularly in places that are hard to reach, including dense jungles, isolated mountain ranges and areas hit by natural disasters like floods, earthquakes, etc. Conventional mapping approaches frequently falter in these conditions, underscoring the necessity for advanced ways to effectively analyse and track these crucial areas. Here, satellite images become useful, providing an aerial view of a region over a period. Using image processing techniques on these images automates the process of understanding the changes on the Earth's surface.

Grenze ID: 01.GIJET.12.2.80_21

The study aims to demonstrate the usage of traditional image processing methods on satellite image data to statistically understand the geospatial variation for two cases: Case-1: Loss of green cover around New Delhi, i.e., analysing the decline of green cover, croplands and grasslands in New Delhi and its surrounding regions due to expanding infrastructure and urban settlements. Case-2: Flood Damage in Kerala, viz., assessing the impact of floods on Kerala's landscape.

Resource mapping using satellite image processing has been extensively studied in recent decades [1]-[5]. Bui B Thien et al. [1] performed image processing using ArcGIS 10.8, including atmospheric correction and the selection of specific Landsat bands for visual interpretation. Vegetation indices were utilised to assess forest vegetation and detect changes in forest cover over the study period. In Ref. [2], for Land Use Land Cover (LULC) analysis, the authors applied five image segmentation techniques, such as threshold-based, edge-based, K-means clustering-based, Otsu's segmentation and Unet with ResUnet on Sentinel-2 satellite images to classify them into ten types of land uses. Ref. [3] aims to inform policymakers and enhance conservation measures for the Sundarbans Mangrove forest region by analysing land cover distribution and temporal changes during 1980-2020 using GIS and remote sensing techniques. The methodology involves acquiring multispectral Landsat satellite data, performing image classification through Maximum Likelihood Classification and evaluating changes in land cover over specified intervals. In a study done by Atiqur Rahman et al. [4], spatial methods such as Shannon's entropy and cellular automata (CA) were integrated with GIS for analysing the urban sprawl of the Hyderabad-Secunderabad region.

This paper presents an algorithm that leverages basic image processing techniques to provide a statistical estimate of geospatial change, serving as an experimental approach to support early-stage policy development and decision-making. This paper is organised as follows: The suggested scheme is explained in Section II. Section III discusses the findings of the experiments and the conclusion in Section IV.

II. DATA AND METHODS

Fig. 1, illustrating the generic block diagram [10], has the following steps: Read a satellite image and convert from RGB to gray-scale(preprocessing), perform segmentation to extract the Region Of Interest (ROI) and then calculate the geographic area of the ROI. Repeat the process for another image of the same region taken at a different time. Compare the areas to find the geospatial changes.

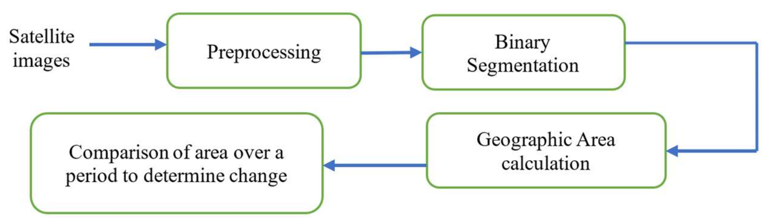

Figure 1. Generic block diagram used in this work

A. Data Source

The satellite image data is obtained from the Landsat Image Gallery provided by NASA [9]. The details are as listed in table I.

B. Preprocessing

A standard process of converting an RGB image to grayscale is used as a preprocessing step, where red (R), green (G), and blue (B)–the three colour channels are reduced to a single intensity channel. This is normally done since colour information is not required during segmentation, thereby reducing memory and increasing computation speed. Using the following formula "(1)," the corresponding gray-intensity value is obtained as a weighted sum of the RGB components according to human visual perception:

$$Gray - value = (0.2989\ x\ R) + (0.5870\ x\ G) + (0.1140\ x\ B) \qquad (1)$$

C. Binary Segmentation

The processing of dividing the image into different regions based on certain similarity is called segmentation. Here, threshold-based image segmentation is utilised to extract the areas of interest. The input to this stage is a gray-scale image $f(x, y)$ obtained in step B. of size M x N and the output is a binary segmented image $g(x, y)$ of the same size, using the following procedure:

- Obtain the pixel value in the input image $p = f(x, y)$
- If $p \geq m$, $g(x, y) = 1\ (white)$
- If $p < m$, $g(x, y) = 0\ (black)$, m is the threshold pixel value determined by manual thresholding and Otsu's thresholding [2].

Repeat the process the for all the pixels in the input image.

TABLE I. SPECIFICS OF THE SATELLITE DATA USED IN THIS WORK

Sl. No.	Case	Image size (pixels)	Metadata [9]
Case - 1	Delhi - Loss of green cover (1989-2018)	4374x3010 JPEG (false colour image)	"Sensor(s): Landsat 5 – TM, Landsat 8 - OLI Data Date: December 5, 1989 - June 5, 2018 Visualization Date: September 26, 2018 Link: https://landsat.visibleearth.nasa.gov/view.php?id=92813"
Case - 2	Kerala Floods 2018 – Before and After	3700x4687, JPEG (false colour image)	"Sensor(s): Landsat 8 - OLI Data Date: August 22, 2018 Visualization Date: August 24, 2018 Link: https://landsat.visibleearth.nasa.gov/view.php?id=92669"

D. Area Calculation

The input to this stage is a segmented binary image $g(x, y)$ obtained in step C. of size M x N. Each connected component in $g(x, y)$ is assigned an ID number. From the resulting labelled image $L(x, y)$, the area is calculated as the number of pixels *N* that belong to the Region of Interest (water body, green cover, etc.).
However, to establish the relationship between pixel measurements and real-world distances, scale factor *S* is determined based on the linear scale provided in the satellite image. This scale factor represents how much each pixel corresponds to in km. The value of *S* is squared, since area is a two-dimensional quantity, giving units like square kilometres per pixel. Then, by counting the total number of pixels *N* in the ROI, multiplying that by the area-per-pixel value (S^2) to estimate the real-world area of a resource which is of interest "(2)".

$$\text{Final geographic area (km}^2\text{)} = NS^2 = \text{ Number of pixels } x \text{ Area per pixel} \qquad (2)$$

E. Area Comparison to Determine Geospatial Variations Over a Period

Two satellite images of the same region over 2 different time periods are used for each case. Steps B to D are performed on both the images. Let area A1 be the area in sq. km. of a region at time t1 and area A2 be the area in sq. km. of the same region at a later time t2. Then geospatial change from t1 to t2 (A1 > A2) can be determined using the below formula "(3)":

$$\text{Percentage change in Geographic area} = \left(\frac{\text{A1} - \text{A}}{\text{A1}}\right) x\ 100 \qquad (3)$$

III. EXPERIMENT AND RESULTS

The experimentation on the above-mentioned cases was carried out using MATLAB R2024b. The Measure Distance option of the Image Viewer app under MATLAB was used to determine the scale factor S. Manual thresholding under the Segmentation App and Otsu's thresholding were used for the segmentation process. In manual thresholding, an appropriate threshold was selected based on a trial-and-error method.
Fig. 2(a) and Fig. 2(b) are the images from the Landsat gallery for case-1. Their corresponding gray-scale images are shown in Fig. 3(a) and Fig. 3(b). Fig. 4(a) and Fig. 4(b) are images obtained after segmenting using a threshold pixel value of m = 137 for the Delhi region in 1989 and m = 145 for the Delhi region in 2018, respectively, using Otsu's method. Here, the white pixels representing the green cover are considered the ROI and the black pixels depict the land regions.
For case-2, Fig. 5(a) and Fig. 5(b) are RGB images. Fig. 6(a) and Fig. 6(b) are the corresponding gray-scale images. Fig. 7(a) and Fig. 7(b) are images obtained after segmenting with a threshold value of m = 76 and m = 95 for the before and after flood images, respectively, using Otsu's method. In this case, the black pixels represent our ROI (water bodies). Fig. 8 shows a sample image showing measurement of the scale factor S. The scaling factor, the geographic area and the percentage change estimated from the binary images using "(2)" and "(3)" are tabulated in table II and table III for the Delhi and Kerala cases, respectively. Further, Fig. 4 is overlaid on Fig. 2 to visually analyse the precision of manual segmentation (Fig. 9), where the land regions are covered by black pixels, while the regions of interest (green cover) appear as is. The threshold was varied manually based on the precision of the segmentation using this overlay.

Figure 2 (a). Original Landsat image of Delhi - 1989

Figure 2 (b). Original Landsat image of Delhi - 2018

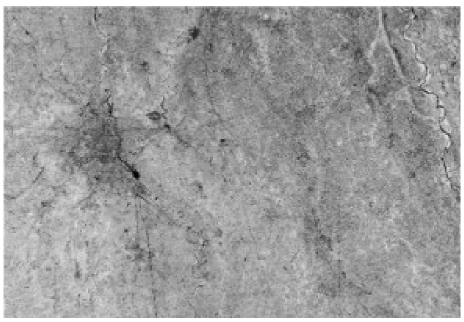

Figure 3 (a). Grayscale image of Delhi - 1989

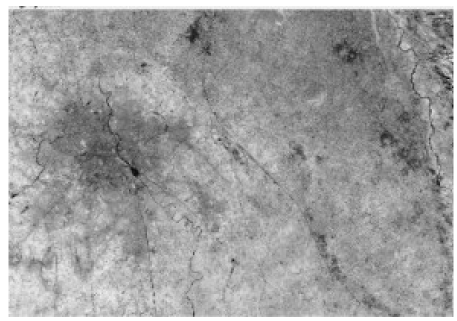

Figure 3(b). Grayscale image of Delhi - 2018, prepared for segmentation

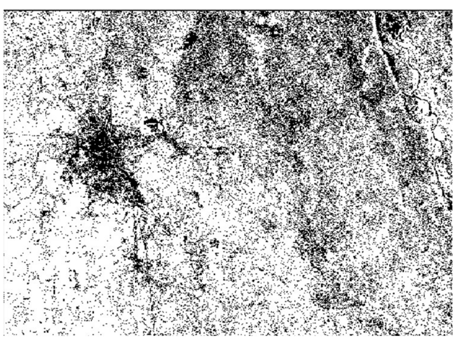

Figure 4 (a). Segmented image of Delhi - 1989

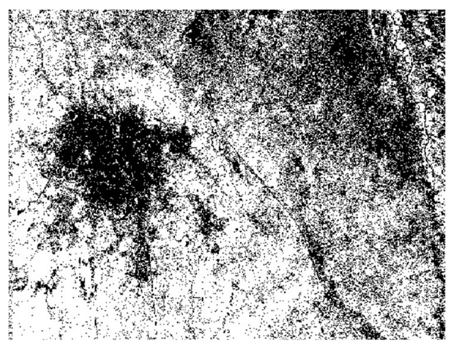

Figure 4(b). Segmented image of Delhi - 2018, black pixels indicate land, while white pixels indicate green cover (ROI)

Figure 5 (a). Original Landsat image of Kerala – Before Floods

Figure 5 (b). Original Landsat image of Kerala – After floods

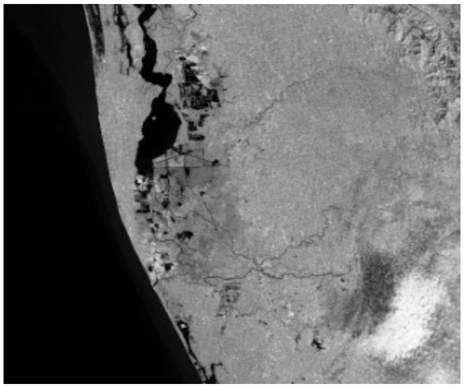

Figure 6 (a). Grayscale image of Kerala – Before Floods

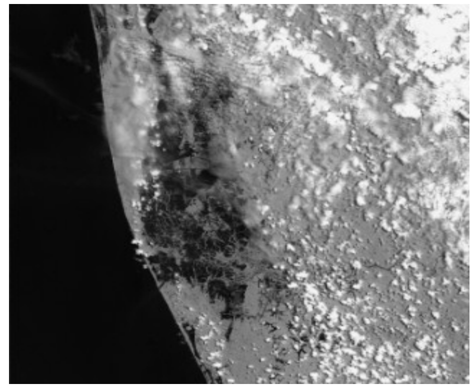

Figure 6(b). Grayscale image of Kerala – After Floods, prepared for segmentation

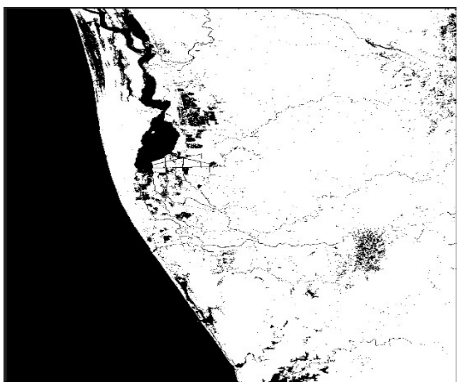

Figure 7 (a). Segmented image of Kerala – Before Floods

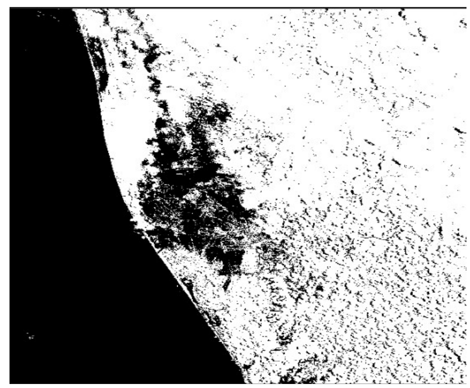

Figure 7 (b). Segmented image of Kerala – After Floods, black pixels indicate water (ROI), while white pixels indicate land

IV. CONCLUSIONS

This work demonstrates how image processing can enhance conventional GIS methods and hence proves satellite imagery to be a valuable and accessible resource for long-term monitoring. Around the national capital, New Delhi, a 23.24% decline in green cover is estimated from the algorithm over a span of 30 years due to rapid urbanisation and increased urban settlements, proving adverse effects on nature. Similarly, around 6.87% of the land was submerged following the 2018 Kerala floods (using manual thresholding). The outcomes are comparable to those derived from segmentation based on Otsu's thresholding. While the results obtained can be further fine-tuned by accessing higher-resolution satellite datasets and precise segmentation by integrating AI/ML algorithms [6], the study is presented as a proof-of-concept demonstration rather than a full-scale geospatial monitoring system, illustrating the potential of simple, approachable methods to capture meaningful geospatial variations.

The results have immediate policy implications in addition to their technical value. To address the ecological loss and achieve SDGs 11 (Sustainable Cities) and 15 (Life on Land), the Delhi case highlights the need for urban design techniques that incorporate green infrastructure (parks, green belts). The flood analysis in Kerala shows how quickly satellite-based change detection may support emergency response, resilience planning and catastrophe preparedness, all of which support SDG 13 (Climate Action). This strategy supports evidence-based policymaking for sustainable development by using low-cost techniques and open-source datasets to give governments, non-governmental organisations and institutions in resource-constrained areas, an approachable framework. In the future, the proposed framework can be extended to other urban regions and to longer multi-year datasets based on the availability of satellite records.

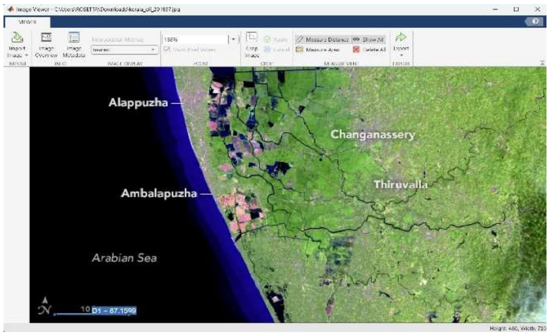

Figure 8. Measuring Scale factor S using MATLAB

Figure 9. Overlay of segments on original image (Case -1)

TABLE II. EXPERIMENTAL RESULTS AND STATISTICAL VALUES OF THE CHANGE IN THE GEOSPATIAL AREA FOR CASE-1: DELHI

Thresholding method	**Scenario**	**Threshold used for segmentation** ***m***	**Scale Factor** ***S***	**Final geographic Area (km²)**	**Percentage change in the Geographic area determined**
Manual thresholding	Delhi Green cover area in 1989	154.6	45 pixels account for 5km	112592	23.24%
	Delhi Green cover area in 2018	144.76		86420	
Otsu's thresholding	Delhi Green cover area in 1989	137		124716.16	16.78%
	Delhi Green cover area in 2018	145		103792.92	

TABLE III. EXPERIMENTAL RESULTS AND STATISTICAL VALUES OF THE CHANGE IN THE GEOSPATIAL AREA FOR CASE -2: KERALA

Thresholding method	**Scenario**	**Threshold used for segmentation** ***m***	**Scale Factor** ***S***	**Final geographic Area (km²)**	**Percentage change in the Geographic area determined**
Manual thresholding	Kerala Water Area-Before Floods	144.7	88 pixels account for 10km	78707.65	6.87%
	Kerala Water Area-After Floods	144.7		84,111.71	
Otsu's thresholding	Kerala Water Area-Before Floods	76		77324.9	15.33%
	Kerala Water Area-After Floods	95		89181.2	

REFERENCES

[1] Thien, B. B., Phuong, V. T., Komolafe, A. A. (2023): "Assessment of forest cover and forest loss using satellite imagesin Thua Thien Hue province, Vietnam". AUC Geographica 58(2), 172–186 https://doi.org/10.14712/23361980.2023.13

[2] Burrewar, Smita & Haque, Mazharul & Haider, Md. (2024), "Enhancing Land Use And Land Cover Analysis Through Image Segmentation Techniques", Journal of Tianjin University Science and Technology, 57. 195-216. DOI: 10.5281/zenodo.13744019

[3] Md. Sharafat Chowdhury, Bibi Hafsa, "Multi-decadal land cover change analysis over Sundarbans Mangrove Forest of Bangladesh: A GIS and remote sensing based approach", Global Ecology and Conservation, Volume 37,2022,e02151,ISSN 2351-9894, https://doi.org/10.1016/j.gecco.2022.e02151

[4] A. Rahman, S. P. Aggarwal, M. Netzband and S. Fazal, "Monitoring Urban Sprawl Using Remote Sensing and GIS Techniques of a Fast Growing Urban Centre, India," in *IEEE Journal of Selected Topics in Applied Earth Observations and Remote Sensing*, vol. 4, no. 1, pp. 56-64, March 2011, doi: 10.1109/JSTARS.2010.2084072

[5] Kumar, M.S. *et al.* (2021), "Monitoring Land Use and Land Cover Changes in Coastal Karnataka. In", Narasimhan, M.C., George, V., Udayakumar, G., Kumar, A. (eds) Trends in Civil Engineering and Challenges for Sustainability. Lecture Notes in Civil Engineering, vol 99. Springer, Singapore https://doi.org/10.1007/978-981-15-6828-2_57

[6] Gowda N Yashaswini, R.V. Manjunath, B Shubha, Punya Prabha, N Aishwarya, H M Manu, "Deep learning technique for automatic liver and liver tumor segmentation in CT images," Journal of Liver Transplantation, Volume 17, 100251, ISSN 2666-9676, (2024) https://doi.org/10.1016/j.liver.2024.100251

[7] Rafael C. Gonzalez and Richard E. Woods. 2006. "Digital Image Processing" (3rd Edition). Prentice-Hall, Inc., USA.
[8] S Jayaraman, S. Esakkirajan, T., Veerakumar, "Digital Image Processing," 1st edn. McGraw Hill Education, 2009.
[9] Landsat Image Gallery https://landsat.visibleearth.nasa.gov/
[10] MATLAB, "Getting Started with Image Processing", [Online Video] Available: https://youtu.be/nAVgUfk-ALE?si=WAmxz0r1K783dkYA